Novel Research in Microbiology Journal (2021), 5(4): 1338-1350
Research Article

(Print) (ISSN 2537-0286)
(Online) (ISSN 2537-0294)
www.nrmj.journals.ekb.eg
DOI: 10.21608/nrmj.2021.190251

Comparative *in vitro* study of the antimicrobial activity of metal-ZnO nanoparticles against several bacterial and fungal pathogens

Mai A. Mwaheb[1]; Laila R. Abd Al Halim[2]; Tarob A. Abdel-Baset[3]; Nada F. Hemeda[4*]

[1]Department of Botany, Faculty of science, Fayoum University, Fayoum 63514, Egypt; [2]Agricultural Microbiology Department, Faculty of Agriculture, Fayoum University, Fayoum 63514, Egypt; [3]Department of Physics, Faculty of Science, Fayoum University, Fayoum 63514, Egypt; [4]Genetics Department, Faculty of Agriculture, Fayoum University, Fayoum 63514, Egypt

[*]Corresponding author E-mail: nfh00@fayoum.edu.eg

Received: 1 July, 2021; Accepted: 16 August, 2021; Published online: 19 August, 2021

Abstract

Nowadays, the use of nanoparticles (NPs) has become useful in the different application fields. The aim of this study was to investigate the *in vitro* antimicrobial potential of metal-ZnO nanoparticles (ZnO NPs) against several bacterial and fungal strains including; *Escherichia coli* (ATCC 25922), *Bacillus cereus* (ATCC 13753), *Staphylococcus aureus* (ATCC 8095), *Pseudomonas aeruginosa* (ATCC10662), *Candida albicans* (ATCC10231) and *Aspergillus niger* (AUMC3663). Results obtained by X-ray diffraction analysis (XRD) showed that the NPs size was in the range of 35.1- 43.7 nm. Images of the scanning electron microscopy (SEM) demonstrated the rod shape nature of the ZnO NPs, and the semi-spherical shapes of the Zn9.7TM0.3O NPs. The effect of different concentrations of ZnO NPs on the *in vitro* growth of the bacterial and fungal strains was evaluated using the agar well diffusion assay. Current results showed that Cd-ZnO NP recorded the highest antimicrobial potency; expressing inhibition zones diameter range of 12- 45 mm, while ZnO NPs demonstrated the least activity exhibiting inhibition zones diameter that ranged from 0- 36 mm. Among all the examined ZnO-NPs, treatment of *E. coli* and *Staph. aureus* cells with Cd-ZnO proved to be the most effective in causing membrane leakage of reducing sugars, protein and DNA recording; 0.41 µg/ ml and 0.38 µg/ ml; 14.91 µg/ ml and 15.98 µg/ ml; 0.81 µg/ ml and 0.96 µg/ ml, respectively. This study emphasized that ZnO NPs could be used as alternative antimicrobial agents to control the bacterial and fungal pathogens. Manipulation of ZnO NPs is ecofriendly; as it reduces the use of the synthetic pesticides and chemical therapeutic agents, which pollute the environment. In the future, *in vivo* application of these NPs necessitates the proof that they have no phytotoxicity and\or cytotoxicity.

Keywords: Metal-ZnO nanoparticles, Antimicrobial activity, Microbial leakage, Reducing sugars, Proteins, DNA

1. Introduction

Metal oxide nanoparticles (NPs) are widely applied in the different fields of research and development (Soosen *et al*., 2009; Kolodziejczak-Radzimska *et al*., 2014). Their properties are determined by the size; shape, composition and crystallinity. NPs are unique as they can be produced with high surface area to volume ratio. The ZnO NPs as antimicrobial agents have excellent stability and\or long shelf life as revealed by Kolodziejczak-Radzimska *et al*., (2014). In addition, they are stable under diverse environmental conditions and fabricate at low temperature (Dhage *et al*., 2005). Metal oxide NPs has distinguished antimicrobial activities, which have opened new frontiers to the biological sciences (Allahverdiyev *et al*., 2011). They have strong toxicity towards a wide range of micro-organisms including bacteria (Huang *et al*., 2008) and fungi (He *et al*., 2011). A previous study conducted by Raghunath and Perumal, (2017) reported that ZnO-NPs possess antimicrobial efficacy against Gram-positive (Guo *et al*., 2015, Gudkov *et al*., 2021) and Gram-negative (Liu *et al*., 2009; Reddy *et al*., 2014, Guo *et al*., 2015; Tiwari *et al*., 2018; Gudkov *et al*., 2021) bacteria, and against bacterial spores (Makhluf *et al*., 2005; Wagner *et al*., 2016). The antibacterial potency of NPs against the pathogenic bacteria such as *E. coli* and *Staph. aureus* are well known (Brayner *et al*., 2006).

Growth of the fungal pathogens in plants is the main cause of considerable economic losses during postharvest handling of grains and fruits. The control of fungal growth is difficult by using the organic substrate, because fungi have developed resistance to many chemical fungicides (Elad *et al*., 1992).

Currently, the structure and composition of synthesized $Zn_{1-x}TM_xO$ (x= 0.03 %), where; TM= Fe, Cd and Mg) have been examined and evaluated. Treatment of microorganisms with ZnO NPs causes membrane leakage of reducing sugars, DNA, proteins and reduces microbial cell viability (Tiwari *et al*., 2018; Yusof *et al*., 2020). The objectives of this study were to synthesize ZnO NPs, check their potent antimicrobial potential against pathogenic bacteria and fungi, and detect their effects on bacterial cellular membrane leakage of reducing sugars, DNA and proteins. The outcomes of our study will help to solve the problem of the microbial chemical resistance, as these metal ZnO NPs will be used to control the pathogenic microorganisms.

2. Material and methods

2.1. Synthesis and preparation of metal-ZnO NPs

All preparation steps of the metal ZnO NPs (Fe, Cd and Mg) and pure ZnO including weighing; grinding, mixing and storage were carried out in an air-filled glove box; where the O_2 and H_2O levels were less than 0.1 µg/ l. Preparation of $Zn_{1-x}TM_xO$ (x= 0.03 %) NPs, where TM= Fe, Cd and Mg was carried out using the co-precipitation technique of Abdel-Baset and Abdel-Hafiez, (2021). During this assay, $ZnSO_4$ and NaOH solutions were prepared individually and then mixed together (according to their molecular weights). The resulting $Zn(OH)_2$ solution was stirred for 2 h at room temperature; followed by heating at 70 °C for 24 h for drying. The dried ingot was heated again for 4 h at 400 °C, and then the resulting powder was left to cool to room temperature to get the pure ZnO NPs. The prepared samples were the oxide dilute magnetic semiconductors; where 25 ml from mixed solutions of $ZnSO_4$ and 3 % of TMs SO_4 at the desired ratio were prepared, and then 25 ml of NaOH solution was added slowly. The above steps were repeated to obtain Zn9.7TM0.3O NPs.

2.2. Characterization of ZnO NPs

2.2.1. X-ray diffraction (XRD) analysis

The size of the obtained NPs was detected using the X-ray diffraction (XRD). Analysis of the samples was performed using a Rigaku miniflex diffractometer

with CuK_{α} radiation (λ = 1.5406 Å), according to Abdel-Baset, (2020). The lattice parameters a and c were calculated using the following relation, according to Karyaoui *et al*., (2015):

$$\frac{1}{d^2_{(hkl)}} = \frac{4}{3}\left[\frac{h^2 + hk + k^2}{a^2}\right] + \frac{l^2}{c^2}$$

Where h, k and l are the Miller Indices, d is inter-planar distance and 'a' and 'c' are lattice parameters, and listed in Table (1).

On the other hand, the average crystalline size (D) was calculated using Debye- Scherrer's equation ($D = k\lambda / (\beta \cos\theta)$) (Abdel-Baset, 2021), where k= 0.94 (a constant), λ is wavelength of X-rays, β is full width at half maximum (FWHM) and θ is the diffraction angle.

2.2.2. Scanning electron microscopy (SEM)

High-resolution scanning electron microscopy (Carl Zeiss sigma 500 VP) was used to determine the NPs size and morphology, in reference to Abdel-Baset, (2021).

2.3. Microbial strains

In this study, strains of *E. coli* (ATCC 25922), *B. cereus* (ATCC 13753), *Staph. aureus* (ATCC 8095), *P. aeruginosa* (ATCC 10662), *C. albicans* (ATCC 10231) and *A. niger* (AUMC 3663) were provided by Assuit University Mycological Center (AUMC), Assuit, Egypt. Nutrient broth (NB) (Himedia Cat. M002- 500G, India) medium was used for general cultivation for all tested bacteria, while potato dextrose agar (PDA) (Difco, USA) was used as a general cultivation medium for the tested yeast and mold fungus.

2.4. Detection of antimicrobial potential of metal ZnO NPs

2.4.1. Preparation of NPs for antimicrobial assay

Metal-ZnO NPs were dissolved in Di-methyl sulfoxide solvent (DIMSO) with different concentration as the following: 5, 10, 15 and 20 µg/ ml (where; 0.5= 5, 1= 10, 1.5 = 15 and 2 = 20 µg/ ml), and DIMSO solvent was used as a control treatment.

2.4.2. Agar well diffusion assay

Agar well diffusion assay was used as described by Wolf and Gibbones, (1996). Briefly, 20 ml of Luria-Bertani agar medium (Atlas and Parks, 1997) was seeded individually with 1% of tested bacterial and fungal suspensions (10^6 cells/ ml) after being cooled to 47˚C, poured into Petri plates and then allowed to solidify. Wells (6 mm diameter) were cut in the solidified agar using a sterile cork borer, and then filled individually with 50 µl of each NPs concentration. Plates were left at 4-5˚C for 2 h to allow diffusion of the NPs suspension and then incubated at 37 °C for 24 h for the bacterial strains, and for 5 d for the fungal strains. After incubation, absence or presence of inhibition zones was recorded, and then the inhibition zone diameters were measured using a calibrated ruler, compared to the control treatment (DMSO). Three replicate plates were used for each treatment.

2.5. Quantitative evaluation of bacterial cellular membrane leakage

The effect of ZnO NPs on causing membrane leakage of reducing sugars, proteins and DNA from the intracellular cytosol of the selected bacterial cells was tested. Flasks containing 100 ml LB broth were inoculated individually with bacterial suspensions (10^6/ ml) of *E. coli* (ATCC 25922) and *Staph. aureus* (ATCC 8095), and with 500 µl of ZnO-NPs (2 mM final concentration). The plates were then incubated at 37 ^{O}C on an orbital shaker at 125 rpm for 24 h. After incubation, the cultures were centrifuged at 10,000 g for 30 min. at 4 ^{O}C. The resulting supernatants were used for determination of the release of bacterial reducing sugars, proteins and DNA. Three replicates were used for each treatment. The reducing sugars were estimated calorimetrically using Di-nitro-salicylic acid assay in reference to Miller, (1959). A blank treatment consisted of dist. water instead of the bacterial filtrate. The absorbance of each sample was

measured individually at 540 nm; using a Jasco V-530 UV/ VIS spectrophotometer (JASCO International CO., LTD., Japan). The total protein was measured using the Biorad Protein Kit II (Biorad) spectrometric assay, according to Bradford, (1976). Following the manufacturer's instruction, the reaction color was stable for one hour. The absorbance was recorded at 595 nm. The linearity was up to 10 grams per decilitre (g/ dl):

The protein concentration (g/ dl) = (A Sample/ A Standard) × 5

Finally, the released DNA (µg/ µl) in each sample was estimated using NanoPhotometer Pearl® (IMPLEN, München, Germany) at 260 nm, according to Li *et al*., (2010); Thombre *et al*., (2016).

2.6. Statistical analysis

All data were expressed as mean values and analysed using general linear model of SPSS. (2007), version 16.0 SPSS company Inc., Chicago, 11, USA, p.444. Mean of the values was compared to the main effects by Duncan's multiple range tests (Duncan, 1955); when significant F values were obtained $p \leq 0.05$.

3. Results

3.1. Synthesis and characterization of ZnO NPs

3.1.1. X-ray diffraction assay

The X-ray diffraction (XRD) pattern of the Zn9.7TM0.3O nanostructure compared to the pure ZnO nanostructure is demonstrated in Fig. (1). Diffraction peaks corresponding to (002) and (100) planes of ZnO as a hexagonal phase were also observed in all samples, but with a different intensity ratio. In addition, no characteristic peaks were observed other than the ZnO peaks, which indicate that the synthesized samples were well crystallized, as shown in Fig. (1). In this study, the recorded crystalline size (D), lattice parameters (a and c) are demonstrated in Table (1).

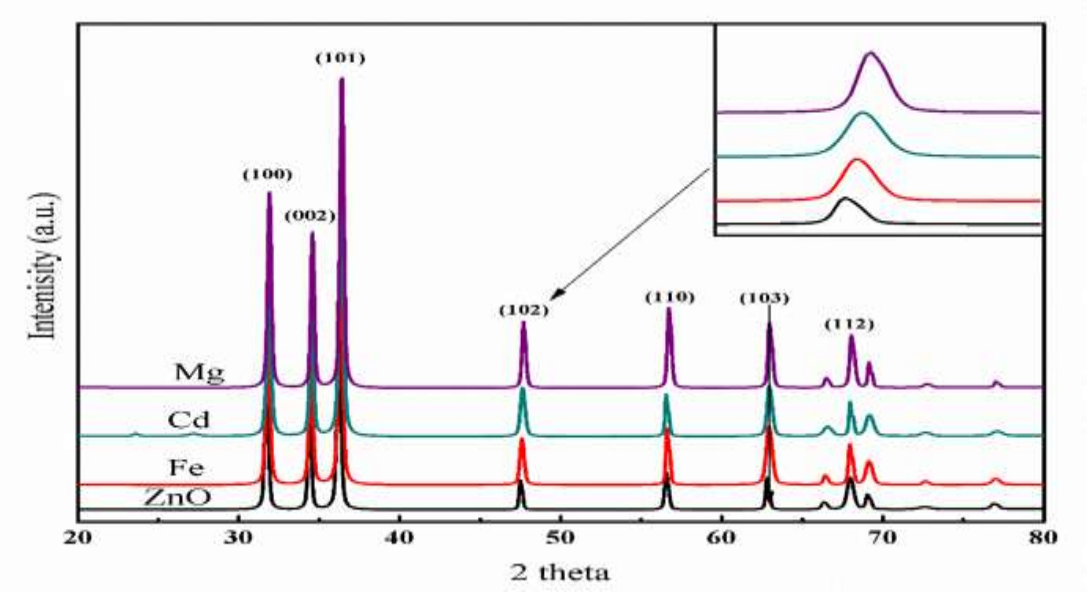

Fig.1: XRD patterns of the pure ZnO, and $Zn_{1-x}TM_xO$ NPs

Table (1): Crystal size, lattice strain and lattice parameters of pure ZnO and Zn9.7TM0.3O NPs

$Zn_{9.7}TM_{0.3}O$	(D)(nm)	*a*	*c*	c/a*
Pure ZnO	43.7	3.2487	5.2033	1.6017
TM= Fe	41.4	3.251	5.209	1.6023
= Cd	38.3	3.25	5.201	1.6003
= Mg	35.1	3.2501	5.2113	1.6034

where *: represents the diagonal axis

The average crystal size decreased with doping, which might be due to the decrease of nucleation of ZnO NPs by doping. Moreover, the slight variation in the lattice parameters probably resulted from substitution of the doped ions with the different ionic radii of Zn. Pure ZnO and Zn9.7TM0.3O NPs were successfully synthesized by the co-precipitation method. From XRD data, the hexagonal wurtzite planes displayed a smaller shift on addition of the metal ions. This effect might be attributed to the different ionic radii of the dopant ions (TMs ions) compared to the ionic radius of Zn. However, on addition of the metal ions the NP size decreased; as revealed by results of the XRD analysis, which are listed in Table (1). This is attributed to the decrease in nucleation; due to the difference between radii of the dopant ions and the Zn ions.

3.1.2. SEM characterization

High resolution scanning electron microscope (HR-SEM) images of the prepared ZnO NPs were used to check their shapes. As demonstrated in Fig. (2a), the SEM image showed the rod shape nature of the ZnO NPs. In addition, the morphology of Zn9.7TM0.3O NPS was studied from the SEM images (Fig. 2: b-d), which showed the semi-spherical shapes of these Zn9.7TM0.3O NPs. The SEM image represents the agglomeration of NPs with narrow particle size distribution.

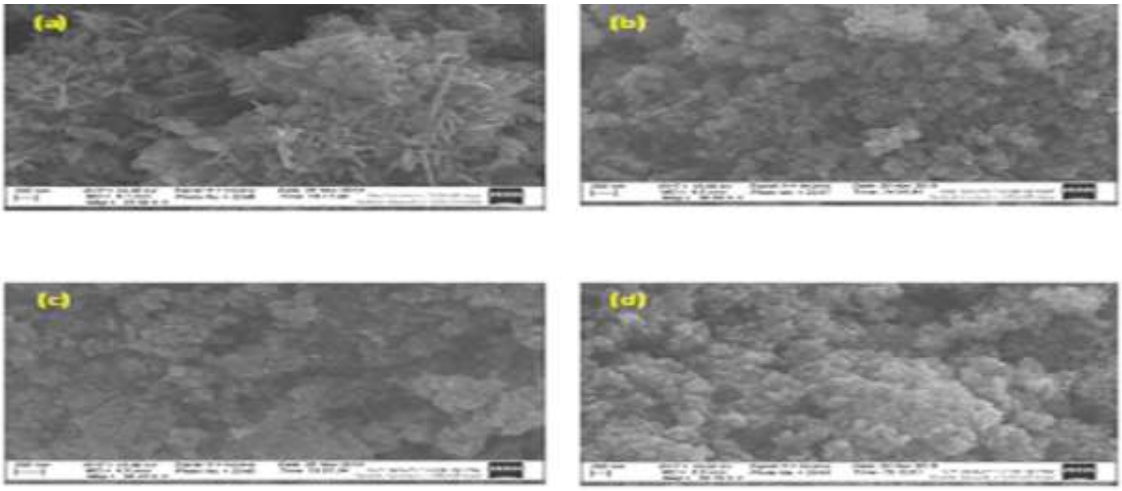

Fig. 2 (a-d): (a) SEM image for ZnO (rod shape); (b, c and d) represent SEM images for $Zn_{1-x}TM_xO$ NPs (semi-spherical shape), where 3% TM concentrations include; Fe, Cd and Mg metals, respectively

3.2. The antibacterial and antifungal efficacy of metal ZnO NPs

Results presented in Table (2) indicated that all the metal ZnO NPs had antimicrobial potential against the tested bacterial and fungal strains manifested through the formation of growth inhibition zones, compared to the control treated with DIMSO only. However, no inhibition zone was recorded for *C. albicans* treated with different concentrations of pure ZnO and Mg-ZnO NPs, compared to the control. Interestingly, the highest antimicrobial potency (inhibition zone diameter of 45 mm) was recorded by Cd-ZnO NP, while ZnO NP presented the least activity (12 mm). In addition, *B. cereus* and *E. coli* strains had moderate sensitivity to the NPs, compared to the other tested bacterial strains. In addition, results revealed that the most effective concentration of NPs was (20 µg/ ml) observed by Cd-ZnO against *B. cereus*, compared to Mg-ZnO and ZnO NPs, as clear in Fig. (3).

Table 2: Antimicrobial activity of metal ZnO NPs against several bacterial and fungal strains using agar well diffusion assay

		Inhibition zones diameter (mm) against the tested bacterial and fungal strains					
		Bacterial strains				**Fungal strains**	
Type of ZnO NPs	Conc. (µg/ml)	*S. aureus*	*B. cereus*	*P.* aeruginosa	*E. coli*	*C. albicans*	*A. niger*
Pure ZnO	Control	0^{h}	0^{i}	0^{j}	0^{f}	0^{e}	0^{g}
	0.5	30^{ef}	12^{gh}	20^{gh}	13^{e}	0^{e}	9^{f}
	1.0	32^{e}	13^{fg}	22^{g}	17^{c}	0^{e}	13^{ef}
	1.5	34^{d}	13^{fg}	25^{f}	17^{c}	0^{e}	15^{e}
	2.0	36^{d}	14^{fg}	30^{de}	19^{b}	0^{e}	17^{d}
Mg-ZnO NPs	Control	0^{h}	0^{i}	0^{j}	0^{f}	0^{e}	0^{g}
	0.5	25^{g}	11^{h}	16^{i}	15^{de}	0^{e}	13^{ef}
	1.0	35^{d}	13^{gh}	18^{h}	16^{cd}	0^{e}	14^{ef}
	1.5	35^{d}	13^{fg}	20^{gh}	16^{cd}	0^{e}	15^{e}
	2.0	35^{d}	22^{b}	20^{gh}	17^{c}	0^{e}	15^{e}
Cd-ZnO NPs	Control	0^{h}	0^{i}	0^{j}	0^{f}	0^{e}	0^{g}
	0.5	30^{f}	20^{c}	29^{e}	17^{c}	7^{d}	19^{c}
	1.0	40^{c}	25^{a}	35^{c}	20^{b}	7^{d}	20^{c}
	1.5	43^{b}	24^{a}	40^{b}	20^{b}	10^{c}	22^{b}
	2.0	45^{a}	25^{a}	45^{a}	25^{a}	12^{b}	25^{a}
Fe-ZnO NPs	Control	0^{h}	0^{i}	0^{j}	0^{f}	0^{e}	0^{g}
	0.5	32^{e}	15^{ef}	20^{gh}	20^{b}	10^{c}	20^{c}
	1.0	35^{d}	16^{e}	25^{f}	20^{b}	10^{c}	24^{a}
	1.5	40^{c}	18^{d}	32^{d}	20^{b}	20^{a}	24^{a}
	2.0	42^{b}	19^{c}	32^{d}	20^{b}	20^{a}	25^{a}

-Results are averages of 3 replicates, and those with the same superscript letters did not differ significantly ($p< 0.05$)

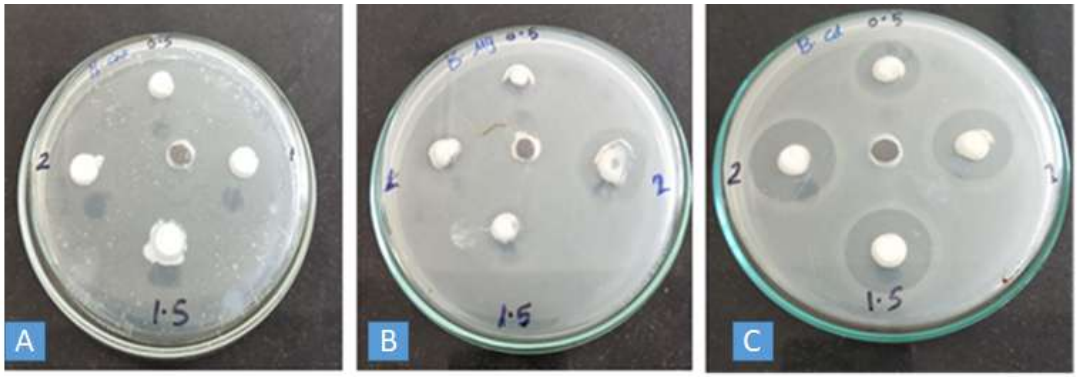

Fig. 3: Agar well diffusion assay for analyzing the *in vitro* effect of metal ZnO-NPs on inhibiting the growth of the tested *B. cereus* strain. Where; (A): Comparative display of chemically synthesized (pure-ZnO) of different conc., (B): Comparative display of chemically synthesized (Mg-ZnO) of different conc., (C) Comparative display of chemically synthesized (Cd-ZnO) of different concentrations. Where the used concentrations were; 0.5= 5, 1= 10, 1.5 = 15 and 2 = 20 µg/ ml

Staph. aureus was strongly affected by all the metal ZnO NPs at all tested concentrations (5, 10, 15, and 20 µg/ ml). On the contrary, we observed that *C. albicans* was resistant to the NPs; as it demonstrated a low inhibition zone diameters of 0 and 12 mm; on treatment with 5 and 15 µg/ ml of Cd-ZnO NPs, respectively. Besides, results showed that treatment of *A. niger* with Cd-ZnO and Fe-ZnO NPs at a concentration of 20 µg/ ml demonstrated significant antifungal potential; expressed through production of a high inhibition zone diameter of 25 mm. Moreover, the most effective concentration of Cd-ZnO and Fe-ZnO NPs was 20 µg/ ml expressing inhibition zone diameters of 45 mm and 42 mm, against *Staph. aureus*.

The current results of this *in vitro* assay showed that Mg-ZnO, Cd-ZnO, Fe-ZnO NPs and pure ZnO had noticeable antibacterial potency against *P. aeruginosa*, exhibiting inhibition zone diameters of; 20, 45, 32 and 30, respectively. All results of the metal ZnO NPs treatments were compared to the control treatment.

From all the above mentioned data, the tested metal ZnO NPs had more significant antibacterial efficacy compared to the antifungal one; especially with the tested strain of *C. albicans*.

3.3. Effect of metal-ZnO NPs on bacterial cellular membrane leakage of reducing sugars, proteins and DNA

Results presented in Table (3) and Fig. (4) demonstrate the effect of metal ZnO-NPs on membrane leakage of reducing sugars, protein and DNA from cells of *E. coli* and *Staph. aureus*. Treatment with Cd-ZnO proved to be the most effective among all the examined ZnO-NPs on causing membrane leakage of reducing sugars, protein, and DNA from *E. coli* and *Staph. aureus*. The recorded membrane leakage of reducing sugars was; 0.27 µg/ ml, 0.41 µg/ ml, 0.19 µg/ ml and 0.22 µg/ ml on treatment of *E. coli* with Fe-ZnO, Cd-ZnO, Mg-ZnO NPs and pure ZnO, respectively. However, leakage of reducing sugars was; 0.31 µg/ ml, 0.38 µg/ ml, 0.19 µg/ ml and 0.28 µg/ ml on treatment of *Staph. aureus* with (Fe-ZnO, Cd-ZnO, Mg-ZnO NPs and pure ZnO, respectively (Fig. 4-A). Similarly, the protein membrane leakage was 13.98 µg/ ml, 14.91 µg/ ml, 12.87 µg/ ml and 13.92 µg/ ml on treatment of *E. coli* with Fe-ZnO, Cd-ZnO, Mg-ZnO NPs and pure ZnO, respectively. Treatment of *Staph. aureus* cells with Fe-ZnO, Cd-ZnO, Mg-ZnO NPs and pure ZnO; scored protein leakage of 14.84 µg/ ml, 15.98 µg/ ml, 12.65 µg/ ml and 13.78 µg/ ml, respectively (Fig. 4-B). The DNA leakage after membrane disruption of *E. coli*

cells was 0.76 µg/ ml, 0.81 µg/ ml, 0.43 µg/ ml and 0.57 µg/ ml on treatment with Fe-ZnO, Cd-ZnO, Mg-ZnO NPs and pure ZnO, respectively. On the other hand; *Staph. aureus* recorded cellular DNA leakage of 0.90 µg/ ml, 0.96 µg/ ml, 0.60 µg/ ml and 0.66 µg/ ml on treatment with Fe-ZnO, Cd-ZnO, Mg-ZnO NPs and pure ZnO, respectively (Fig. 4-C). The control represented the non-treated bacterial cultures.

Results presented in Table (3) showed that treatment of *E. coli* and *Staph. aureus* with NPs caused cellular bacterial permeability leakage of reducing sugars, proteins and DNA. Accordingly, the use of NPs will be an important factor in preventing growth of the different bacterial pathogens, and displace the use of the deleterious synthetic bactericides that pollute the environment.

Table 3: The effect of metal ZnO-NPs on causing cellular membrane leakage of protein, reducing sugar and DNA from the tested bacterial strains

Treatment with NPs	**Membrane leakage of**		
	Protein	Reducing sugars	DNA
Control *E. coli*	10.83^{e}	0.15^{e}	0.30^{e}
E. coli + Fe-ZnO	13.98^{b}	0.27^{b}	0.76^{b}
E. coli + Cd-ZnO	14.91^{a}	0.41^{a}	0.81^{a}
E. coli + Mg-ZnO	12.87^{d}	0.19^{d}	0.43^{d}
E. coli + pure ZnO	13.92^{c}	0.22^{c}	0.57^{c}
Control *Staph. aureus*	11.63^{e}	0.15^{e}	0.57^{e}
Staph. + Fe-ZnO	14.84^{b}	0.31^{b}	0.9^{b}
Staph.+ Cd-ZnO	15.98^{a}	0.38^{a}	0.96^{a}
Staph.+ Mg-ZnO	12.65^{d}	0.2^{d}	0.60^{d}
Staph.+ pure ZnO	13.78^{c}	0.28^{c}	0.66^{c}

-Results are averages of 3 replicates, and those with the same superscript letters did not differ significantly ($p< 0.05$)

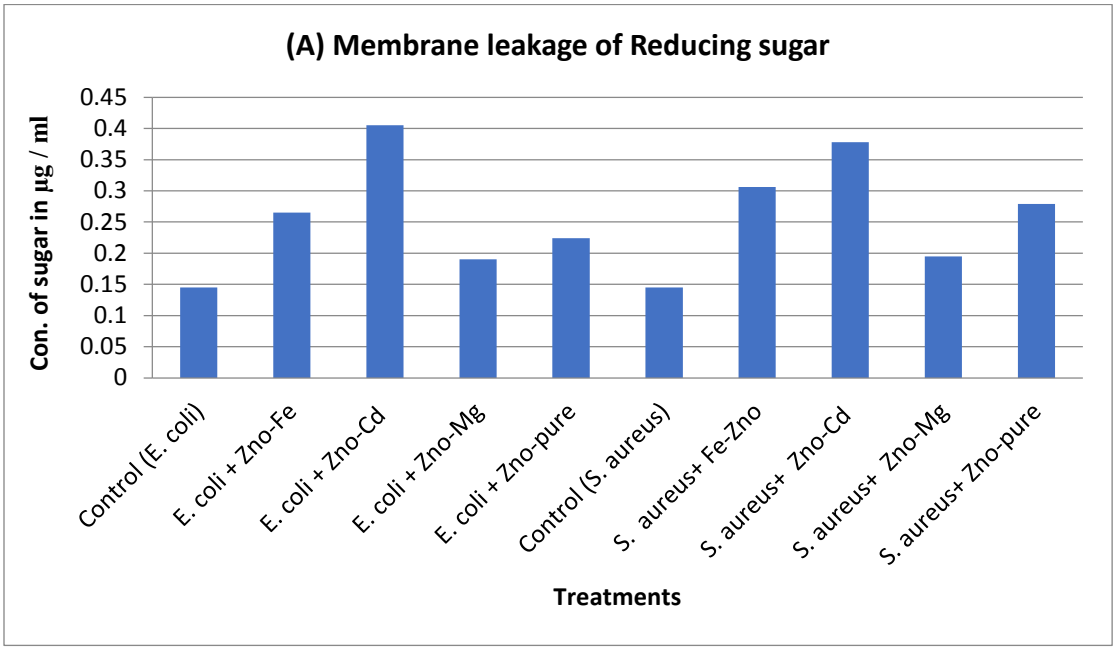
(A) Membrane leakage of Reducing sugar
Con. of sugar in µg / ml
0.45
0.4
0.35
0.3
0.25
0.2
0.15
0.1
0.05
0
Control (E. coli)
E. coli + Zno-Fe
E. coli + Zno-Cd
E. coli + Zno-Mg
E. coli + Zno-pure
Control (S. aureus)
S. aureus+ Fe-Zno
S. aureus+ Zno-Cd
S. aureus+ Zno-Mg
S. aureus+ Zno-pure
Treatments

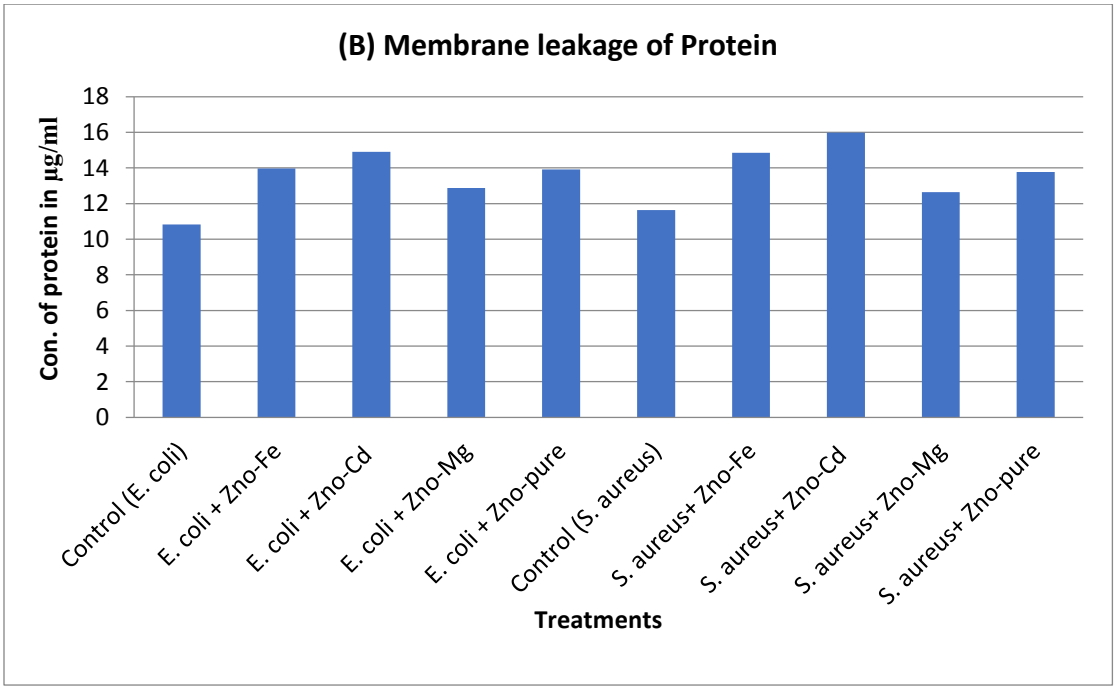
(B) Membrane leakage of Protein
Con. of protein in µg/ml
18
16
14
12
10
8
6
4
2
0
Control (E. coli)
E. coli + Zno-Fe
E. coli + Zno-Cd
E. coli + Zno-Mg
E. coli + Zno-pure
Control (S. aureus)
S. aureus+ Zno-Fe
S. aureus+ Zno-Cd
S. aureus+ Zno-Mg
S. aureus+ Zno-pure
Treatments

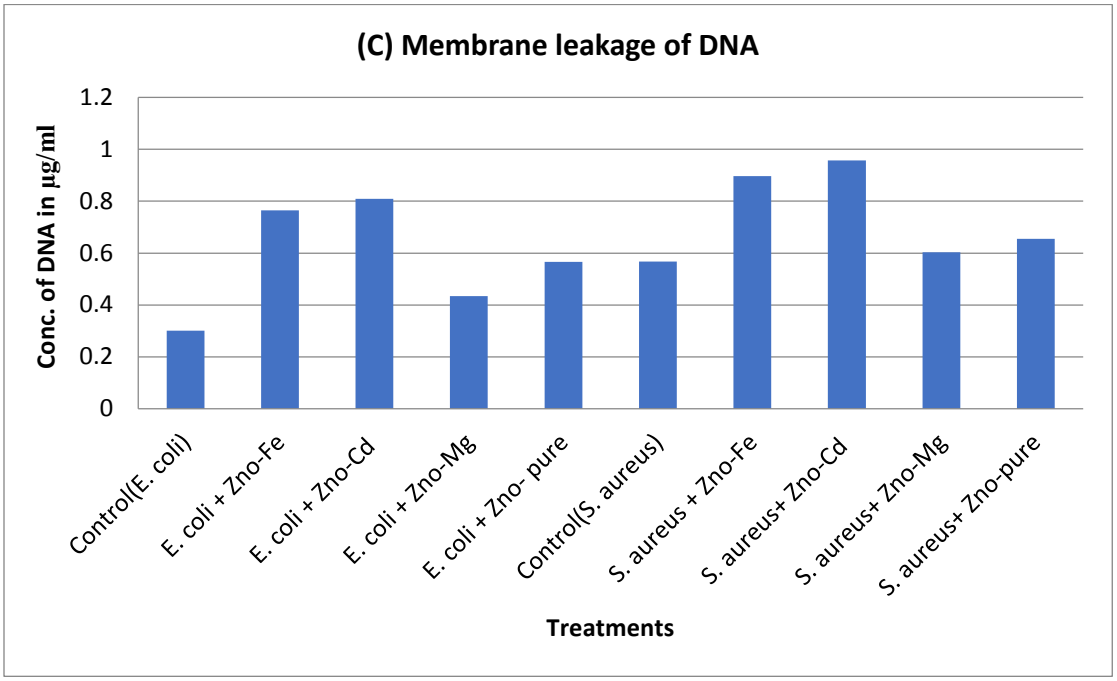

Fig. 4: Microbial membrane leakage from cells of *E. coli* and *Staph. aureus* after treatment with chemically synthesized ZnO-NPs. Comparative quantitative display of leakage of; (A): reducing sugar; (B): protein and (C): DNA

4. Discussion

The current results indicated that the chemically synthesized ZnO NPs were well crystallized. The average crystal size of the NPs detected using the XRD analysis decreased with doping, due to the decrease of nucleation of ZnO NPs by doping, in accordance with Abdel-Baset and Abdel-Hafiez, (2021). The slight variation in the lattice parameters resulted from substitution of the doped ions with different ionic radii of Zn, which led to improving their properties without changing the host (ZnO) crystal structure over a wide dopant concentration, similar to results of the recent study conducted by Abdel-Baset and Abdel-Hafiez, (2021).

The XRD pattern suggested that pure ZnO exhibits a hexagonal wurtzite structure belonging to the C46v space group (P63mc). ZnO is indexed and uses a standard JCPDS file for NPs (JCPDS 36-1451) with a preferred (101) orientation (Abdel-Baset and Belhaj, 2021). In agreement with Abdel-Baset and Abdel-Hafiez, (2021), the hexagonal wurtzite planes displayed a small shift with the addition of metal ions, which might be attributed to the different ionic radii of the dopant ions with the ionic radius of Zn. On the other hand, on addition of the metal ions the particle size decreased, because of the decrease in the nucleation and subsequent growth rate related to the difference between the dopant ions and the Zn ions.

The diffraction peaks corresponding to (002) and (100) planes of ZnO as a hexagonal phase were also observed in all samples, but with a different intensity ratio. In addition, no characteristic peaks were observed other than the ZnO peaks, which indicate that the synthesized samples were well crystallized. On the other hand, the peaks were slightly shifted toward higher angle with doping, which might be attributed to the different ionic radii of the dopant ions with the ionic radius of Zn as proposed by Irshad *et al*., (2018).

The SEM images showed the rod shape nature of pure ZnO; the presence of Zn9.7TM0.3O NPs samples in a semi-spherical shape, which represents the agglomeration of particles with narrow particle size distribution. The current results indicated that all metal ZnO NPs had antimicrobial activity against all the tested bacterial and fungal strains, compared to the control. Nanotechnology is increasingly used to control pathogens as an alternative to antibiotics (Wang *et al*., 2017). These NPs have significantly high antibacterial potential, as reported by Gudkov *et al*., (2021). In addition, the present results confirmed that bacterial treatment with Cd-ZnO was the most effective among all the examined ZnO-NPs; causing membrane leakage of reducing sugars, protein and DNA from cells of *E. coli* and *Staph. aureus*. The NPs are less prone to promoting resistance in microbial pathogens than the antibiotics (Wang *et al*., 2017). The ZnO-NPs could be developed as alternative therapeutics against the pathogenic microorganisms. Direct interaction of the ZnO NPs with the microbial cell cause damages of the cell membrane integrity, which leads to cell rupture and leakage of intracellular contents (Yusof *et al*., 2020). One mechanism of the antimicrobial action of ZnO NPs is the intracellular responses such as the cell membrane damage (Su-Eon Jin and Hyo-Eon Jin, 2021). The use of ZnO NPs as nano-microbicides is ecofriendly and will increase both the crop production and the national income. Moreover, NPs act as powerful and new drug substitutes against the multi-drug resistant bacteria (i.e. *E. coli* and *Staph. aureus*) and the pathogenic fungi (*C. albicans*), in agreement with results of the previous study of Abd Elkodous et al., (2019). However, the phytotoxicity and cytotoxicity of these NPs should be checked; respectively, before in vivo wide scale application in the field as nano-microbicides, and\or their use in treatments of multidrug resistant pathogenic microorganisms.

Conclusion

The use of ZnO NPs could be alternative therapeutics against the bacterial and fungal pathogens; as they decrease plant and animals infestation and increase crop production. Manipulation of metal ZnO NPs on a wide scale in the field preserve the environment, and provide safe food in larger quantities and at lower costs. However, the phytotoxicity and cytotoxicity of these metal ZnO NPs should be tested before their *in vivo* use on a wide scale in the fields.

Conflict of interest

The authors declare that there is no conflict of interests related to this manuscript.

Acknowledgements

The authors are grateful to the Faculty of Agriculture and Faculty of Science, Fayoum University, Egypt, for providing laboratory facilities to carry out this study.

Funding source

This study did not receive any fund.

Ethical approval

Non-applicable.

5. References

Abdel-Baset, T. (2021). Structure, Optical, Dielectric and Magnetic Properties of Zn0.99M0.01O (M= Ni, Fe and Cd) nanoparticles. Journal of Superconductivity and Novel Magnetism. 34: 1259-1267.

Abdel-Baset, T. and Abdel-Hafiez, M. (2021). Effect of metal dopant on structural and magnetic properties of ZnO nanoparticles. Journal of Materials Science: Materials in Electronics. 32: 16153-16165.

Abdel-Baset, T. and Belhaj, M. (2021). Structural characterization, dielectric properties and electrical Conductivity of ZnO nanoparticles synthesized by co-precipitation route. Physica. B 616: 413130.

Abdel-Baset, T.A. (2020). Dielectric and optical properties of PVA/PAN doped TiO_2 NPs**.** Journal of

Materials Science: Materials in Electronics. 31: 15960-15967.

Abd Elkodous, M.; El-Sayyad, G.S.; Abdelrahman, I.Y.; El-Bastawisy, H.S.; Mohamed, A.E.; Mosallam, F.M.; Nasser, H.A. ; Gobara, M.; Baraka, A.; Elsayed, M.A. and El-Batal, A. I. (2019). Therapeutic and diagnostic potential of nanomaterials for enhanced biomedical applications. Colloids and Surfaces B: Biointerfaces. 180: 411-428.

Allahverdiyev, A.M.; Kon, K.V.; Abamor, E.S.; Bagirova, M. and Rafailovich, M. (2011). Coping with antibiotic resistance: combining nanoparticles with antibiotics and other antimicrobial agents. Expert Review of Anti-infective. 9: 1035-1052.

Atlas, R. and Parks, L.C. (1997). Handbook of Microbiological Media. 2nd edition, CRC press. 1706.

Bradford, M.M. (1976). A rapid and sensitive method for the quantitation of microgram quantities of protein utilizing the principle of protein-dye binding. Analytical Biochemistry. 72: 248-254.

Brayner, R.; Ferrari-Iliou, R.; Brivois, N.; Djediat, S.; Benedetti, M.F. and Fiévet, F. (2006). Toxicological impact studies based on *Escherichia coli* bacteria in ultrafine ZnO nanoparticles colloidal medium. Nano Letters. 6: 866-870.

Dhage, S.; Pasricha, R. and Ravi, V. (2005). Synthesis of fine particles of ZnO at 100 C. Materials Letters. 59: 779-781.

Duncan, D. (1955). Multiple Range and Multiple F Tests. Biometrics. 11(1): 1-42.

Elad, Y.; Yunis, H. and Katan, T. (1992). Multiple fungicide resistance to benzimidazoles, dicarboximides and diethofencarb in field isolates of *Botrytis cinerea* in Israel. Plant Pathology. 41: 41-46.

Gudkov, S.V.; Burmistrov, D.E.; Serov, D.A.; Rebezov, M.B.; Semenova, A.A. and Lisitsyn, A.B. (2021). A Mini Review of Antibacterial Properties of ZnO Nanoparticles. Frontiers in Physics. 9: 641481.

Guo, B.L.; Han, P.; Guo, L.C.; Cao, Y.Q.; Li, A.D.; Kong, J.Z. et al. (2015). The antibacterial activity of Ta-doped ZnO nanoparticles. Nanoscale Research Letters. 10: 336.

He, L.; Liu, Y.; Mustapha, A. and Lin, M. (2011). Antifungal activity of zinc oxide nanoparticles against *Botrytis cinerea* and *Penicillium expansum*. Microbiological Research. 166: 207-215.

Huang, Z.; Zheng, X.; Yan, D.; Yin, G.; Liao, X.; Kang, Y. et al. (2008). Toxicological effect of ZnO nanoparticles based on bacteria. Langmuir. 24: 4140-4144.

Irshad, K.; Khan, M.T. and Murtaza, A. (2018). Synthesis and characterization of transition-metals-doped ZnO nanoparticles by sol-gel auto-combustion method. Physica B. 543: 1-6.

Karyaoui, M.; Mhamdi, A.; Kaouach, H.; Labidi, A.; Boukhachem, A.; Boubaker, K.; Amlouk, M. and Chtourou, R. (2015). Some physical investigations on silver-doped ZnO sprayed thin films. Materials Science in Semiconductor Processing. 30: 255-262.

Kolodziejczak-Radzimska, A. and Jesionowski, T. (2014). Zinc Oxide-From Synthesis to Application. Materials. 7: 2833-2881.

Li, W.R.; Xie, X.B.; Shi, Q.S.; Zeng, H.Y.; You-Sheng, O.Y. and Chen, Y.B. (2010). Antibacterial activity and mechanism of silver nanoparticles on *Escherichia coli*. Applied Microbial and Cell Physiology. 85: 1115-1122.

Liu, Y.; He, L.; Mustapha, A.; Li, H.; Hu, Z.Q. and Lin, M. (2009). Antibacterial activities of zinc oxide nanoparticles against *Escherichia coli* O157: H7. Journal of Applied Microbiology. 107: 1193-1201.

Makhluf, S.; Dror, R.; Nitzan, Y.; Abramovich, Y.; Jelinek, R. and Gedanken, A. (2005). Microwave-assisted synthesis of nanocrystalline MgO and its use as a bacteriocide. Advanced Functional Materials. 15: 1708-1715.

Miller, G.L. (1959). Use of dinitrosalicylic acid reagent for determination of reducing sugar. Analytical Chemistry. 31: 426-428.

Raghunath, A. and Perumal, E. (2017). Metal oxide nanoparticles as antimicrobial agents: a promise for the future. International Journal of Antimicrobial Agents. 49: 137-152.

Reddy, L.S.; Nisha, M.M.; Joice, M. and Shilpa, P.N. (2014). Antimicrobial activity of zinc oxide (ZnO) nanoparticle against *Klebsiella pneumoniae*. Pharmaceutical Biology. 52: 1388-1397.

Soosen, S.M.; Bose, L. and George, K.C. (2009). Optical Properties of ZnO Nanoparticles. Academic Review. 16(1-2): 57-65.

Su-Eon Jin and Hyo-Eon Jin. (2021). Antimicrobial Activity of Zinc Oxide Nano/Microparticles and Their Combinations against Pathogenic Microorganisms for Biomedical Applications: From Physicochemical Characteristics to Pharmacological Aspects. Nanomaterials. 11(2): 263**.**

Thombre, R.S.; Shinde, V.; Thaiparambil, E.; Zende, S. and Mehta, S. (2016). Antimicrobial activity and mechanism of inhibition of silver nanoparticles against extreme halophilic archaea. Frontiers in Microbiology. 7: 1424.

Tiwari, V.; Mishra1, N.; Gadani, K.; Solanki, P.S.; Shah, N.A. and Tiwari, M. (2018). Mechanism of Anti-bacterial Activity of Zinc Oxide Nanoparticle Against Carbapenem-Resistant *Acinetobacter baumannii*. Frontiers in Microbiology. 9: 1218.

Wagner, G.; Korenkov, V.; Judy, J.D. and Bertsch, P.M. (2016). Nanoparticles composed of Zn and ZnO inhibit *Peronospora tabacina* spore germination *in vitro* and *P. tabacina* Infectivity on Tobacco Leaves. Nanomaterials (Basel) 6: 50.

Wang, L.; Chen, H. and Shao, L. (2017). The antimicrobial activity of nanoparticles: present situation and prospects for the future. International Journal of Nanomedicine. 12: 1227-1249.

Wolf, C.E. and Gibbones, W.R. (1996). Improved method for quantification of the bacteriocin nicin. Journal of Applied Bacteriology. 80: 453-457.

Yusof, H.M.; Abdul Rahman, N.; Mohamad, R.; Zaidan, U.H. and Samsudin, A.A. (2020). Biosynthesis of zinc oxide nanoparticles by cell‐biomass and supernatant of *Lactobacillus plantarum* TA4 and its antibacterial and biocompatibility properties. Scientific Reports. 10 (1):19996.